Stem Cell Reports

Article



-OPEN ACCESS

Physiological calcium combined with electrical pacing accelerates maturation of human engineered heart tissue

Shi Shen,^{1,6} Lorenzo R. Sewanan,^{2,6} Stephanie Shao,¹ Saiti S. Halder,¹ Paul Stankey,^{3,4} Xia Li,¹ and Stuart G. Campbell^{1,5,*}

¹Department of Biomedical Engineering, Yale University, 55 Prospect St. MEC 211, New Haven, CT 06511, USA

SUMMARY

Human-induced pluripotent stem cell-derived cardiomyocytes (hiPSC-CMs) have wide potential application in basic research, drug discovery, and regenerative medicine, but functional maturation remains challenging. Here, we present a method whereby maturation of hiPSC-CMs can be accelerated by simultaneous application of physiological Ca^{2+} and frequency-ramped electrical pacing in culture. This combination produces positive force-frequency behavior, physiological twitch kinetics, robust β -adrenergic response, improved Ca^{2+} handling, and cardiac troponin I expression within 25 days. This study provides insights into the role of Ca^{2+} in hiPSC-CM maturation and offers a scalable platform for translational and clinical research.

INTRODUCTION

Despite their immense potential for clinical and basic science applications, stem-cell derived cardiomyocytes (iPSC-CMs) have been limited by their relatively immature phenotypes. Their structural, metabolic, and molecular characteristics are often similar to those of neonatal cardiomyocytes (Feric and Radisic, 2016; Ma et al., 2018; Robertson et al., 2013; Sewanan and Campbell, 2020; Tiburcy et al., 2017). Crucially, immature protein isoforms manifest as alterations in critical aspects of adult cardiac physiology, notably twitch kinetics, Ca²⁺ handling, the force-length relationship, the force-frequency relationship, and beta-adrenergic responsiveness.

Recent work has made strides toward enhancing iPSC-CM maturation through the use of complex media formulations and electromechanical stimulation protocols (Feyen et al., 2020; Funakoshi et al., 2021; Gomez-Garcia et al., 2021; de Lange et al., 2021; Pakzad et al., 2021; Ronaldson-Bouchard et al., 2018; Zhao et al., 2019). For example, in a decellularized matrix-based engineered heart tissue (EHT), β-myosin heavy chain expression levels of >90% (similar to adult human myocardium) can be obtained by subjecting EHTs to constant electrical pacing in an isometric format (Ng et al., 2021). Meanwhile, protocols that resulted in advanced electrophysiological and Ca²⁺-related maturity used electrical pacing with progressive rate increase over time (Ronaldson-Bouchard et al., 2018; Zhao et al., 2019). Such studies point to important roles for progressive electrical pacing, a tissue format that allows the formation of cardiac syncytia,

proper mechanical substrate (matrix), and appropriate mechanical loading.

As far as we are aware, the role of Ca²⁺ in maturation of EHTs has not been systematically explored. This is surprising, given that development of Ca2+ handling behavior precedes and may even drive cardiomyocyte differentiation through a variety of downstream Ca²⁺-dependent pathways (Louch et al., 2015; Tyser et al., 2016). The RPMI basal media frequently used for growing iPSC-CMs contains less than one-third the concentration of free Ca²⁺ seen physiologically. It seems possible that this low Ca²⁺ concentration is insufficient to spur full maturation of Ca²⁺ handling and excitation-contraction machinery of the cardiomyocyte. We hypothesized that providing physiological Ca²⁺ to EHT grown under isometric conditions with progressive electrical pacing would accelerate and enhance functional maturation, representing a simple, scalable advance in the maturation of iPSC-CMs. As metrics of myocardial maturation, we focused on the EHT force-frequency response (FFR), post-rest potentiation, and isometric twitch force behavior.

RESULTS

To test whether physiological levels of Ca^{2+} alone could alter functional maturation, we compared two groups of EHTs: one was cultured in high-glucose DMEM (nominally 1.8 mM free Ca^{2+}) and the other in high-glucose RPMI (nominally 0.42 mM free Ca^{2+}), with neither receiving ramp pacing (high- Ca^{2+} non-paced [HC-NP] and



²Department of Medicine, Columbia University Irving Medical Center, New York, NY, USA

³Wyss Institute for Biologically Inspired Engineering, Harvard University, Boston, MA, USA

⁴John A. Paulson School of Engineering and Applied Sciences, Harvard University, Cambridge, MA, USA

⁵Department of Cellular and Molecular Physiology, Yale University, New Haven, CT, USA

⁶These authors contributed equally

^{*}Correspondence: stuart.campbell@yale.edu https://doi.org/10.1016/j.stemcr.2022.07.006



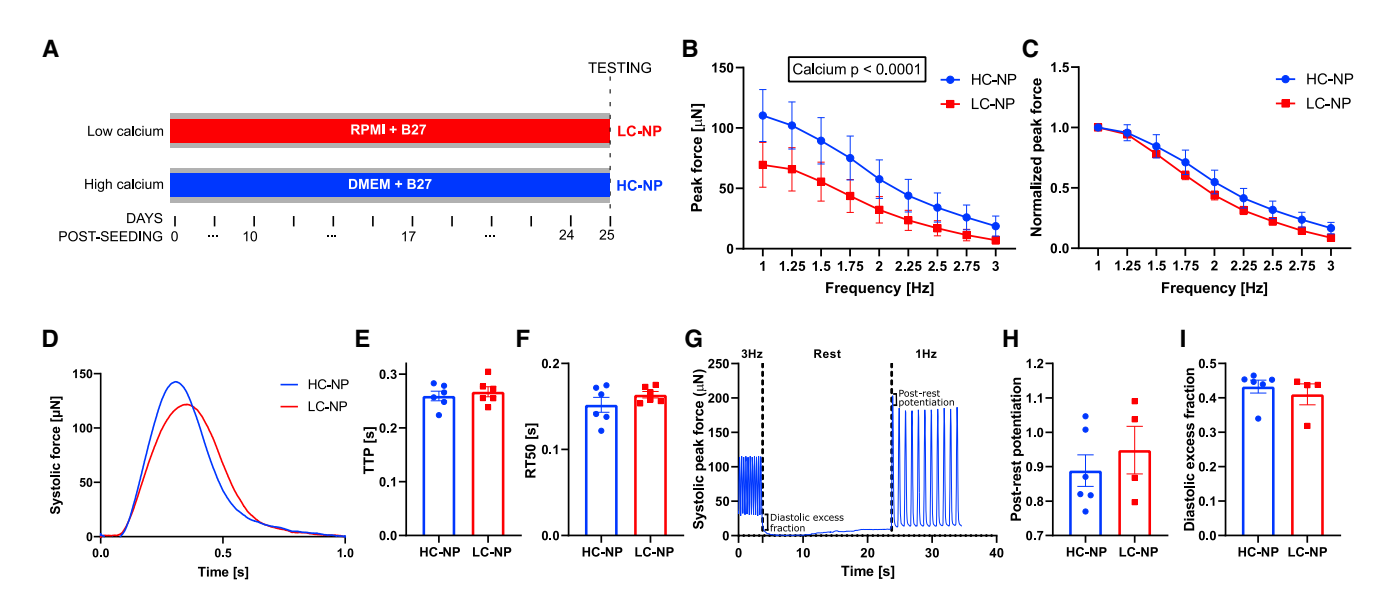


Figure 1. Physiological level Ca^{2+} alone increases contractile force but does not improve overall functional maturation profile (A) Experimental design schematic of HC-NP and LC-NP groups. (B and C), (E and F) both n = 6, (H and I) HC-NP n = 6, LC-NP n = 4. All data came from one differentiation batch.

- (B) Unnormalized force-frequency relationship (FFR).
- (C) Normalized FFR.
- (D) Representative twitches of the two groups at 1 Hz.
- (E) TTP at 1 Hz.
- (F) RT50 at 1 Hz.
- (G) Representative HC-NP post-rest potentiation data sequence.
- (H) Post-rest potentiation.
- (I) Diastolic excess fraction. two-way ANOVA with repeated measures (B and C) and unpaired two tailed t-tests (E, F, H, and I) were performed. two-way ANOVA p = n.s. (B and C), and t-tests p = n.s. (E, F, H, and I).

low-Ca²⁺ non-paced (LC-NP) (Figure 1A). After 24 days in culture, EHTs were mounted in a mechanical testing apparatus and isometric force was measured in response to a pacing frequency staircase from 1 to 3 Hz in 0.25-Hz increments. The raw FFR showed higher systolic peak forces for HC-NP group across 1–3 Hz (Ca²⁺ p < 0.0001), but FFR in both groups was negative overall (Figure 1B). A closer look at the FFR with normalized systolic peak forces revealed a marginal improvement in HC-NP, although both were still highly negative (Figure 1C). Physiological Ca²⁺ alone also failed to significantly improve twitch kinetics (Figures 1D–1F).

Post-rest potentiation was assessed by pacing tissues at 3 Hz, pausing stimulus for 15 s, and then restarting pacing at 1 Hz (Figures 1G–1I). The ratio between the first twitch and the subsequent twitches at 1 Hz is an indirect measure of sarcoplasmic reticulum Ca²⁺-handling capacity (Pieske et al., 1996). The diastolic excess fraction, or the relationship between the diastolic force at 3 Hz and at rest was correlated with tissues' ability to inhibit contraction at low Ca²⁺ levels (Varian et al., 2009). The HC-NP group exhibited improvements in neither post-rest potentiation

nor diastolic excess fraction compared to the LC-NP group (Figures 1G–1I).

To test our hypothesis that near-physiological levels of free Ca²⁺ in culture media in conjunction with ramp pacing would functionally improve EHTs, we again divided the tissues into high-glucose DMEM and high-glucose RPMI culture groups. This time, 10 days after seeding both groups were subjected to a 2-week, 2- to 4-Hz ramp up pacing protocol (Figure 2A) in a custom pacing bioreactor (Figure 2B) and then FFR was tested 1 day after ramp completion. Representative raw twitches demonstrated that the high-Ca²⁺ ramp-paced group (HC-RP) tissues had positive FFR behavior up to 2 Hz, while the low-Ca²⁺ ramp-paced group (LC-RP) tissues maintained purely negative FFR (Figure 2C).

Both groups maintained a similar twitch force magnitude at 1 Hz pacing rate, but diverged significantly in terms of both raw and normalized force as frequency was increased from 1 to 3 Hz (Figures 2D and 2E). HC-RP EHTs also displayed significantly faster time to peak (TTP, Figure 2F) across the entire frequency range and time to 50% relaxation (RT50) (Figure 1G) up to 2 Hz. Representative records and summary data at 1 Hz clearly showed the overall



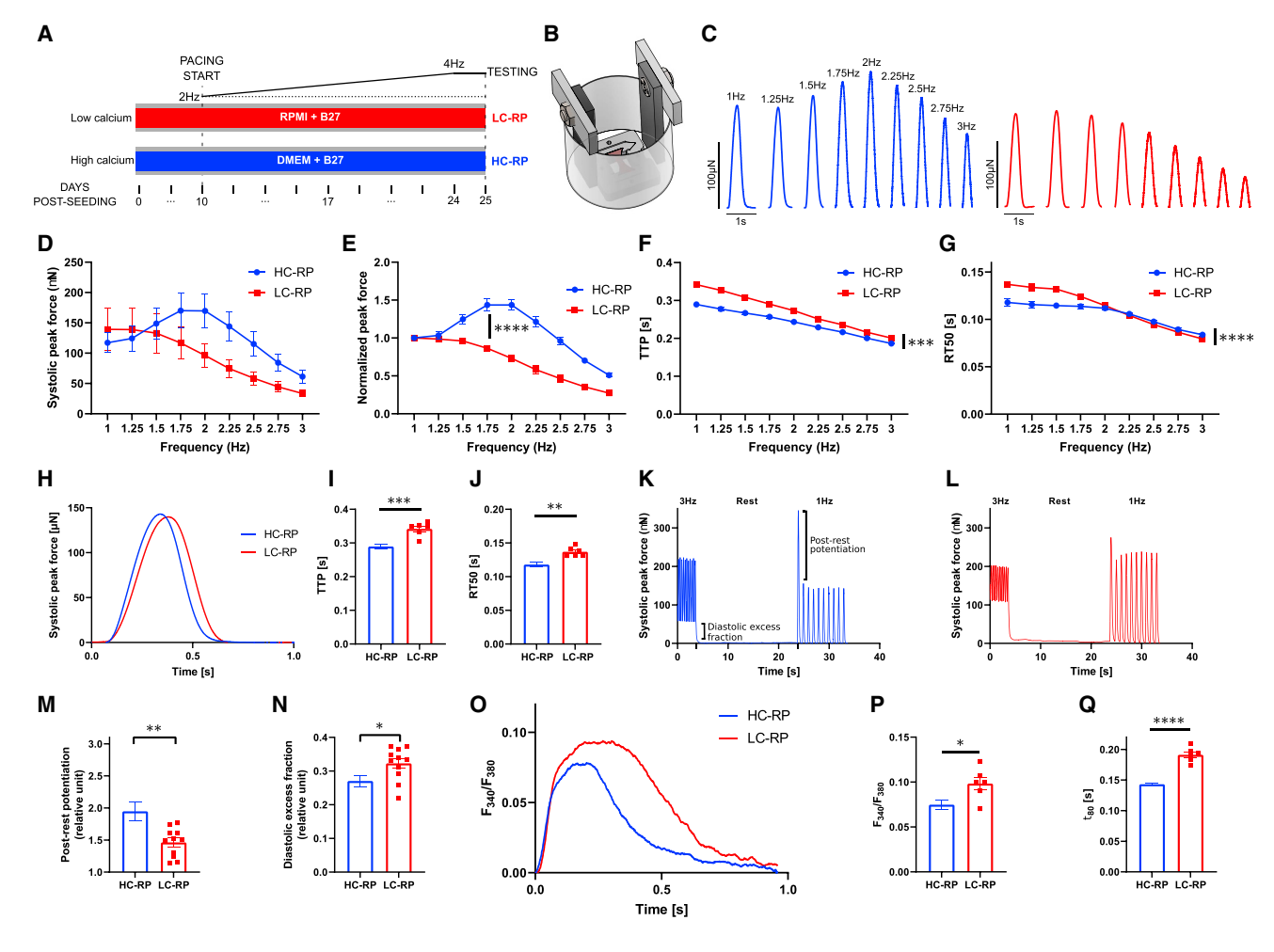


Figure 2. Physiological level Ca2+ and pacing result in functional improvement

- (A) Experimental design of high-Ca2+ ramp-paced (HC-RP) and low-Ca2+ ramp-paced (LC-RP) groups with 2-week continuous 2-4 Hz ramp pacing. C-J n = 6 for both groups from a single differentiation batch. M-N HC-RP n = 8, LC-RP n = 11 from two batches. 0-P n = 6 for both groups from two batches.
- (B) SOLIDWORKS drawing of the pacing apparatus for individual tissues cultured in a 12-well plate.
- (C) Representative force-frequency relationship (FFR) for HC-RP (blue) and LC-RP (red) groups respectively from 1–3 Hz with 0.25 Hz increments.
- (D) Unnormalized FFR.
- (E) Normalized FFR (p < 0.0001).
- (F) Time to peak (TTP) at 1-3 Hz (p = 0.0003).
- (G) Time to 50% relaxation (RT50) at 1-3 Hz (p < 0.0001).
- (H) Representative twitches at 1 Hz.
- (I) Time to peak (TTP) at 1 Hz (p = 0.0009).
- (J) Time to 50% relaxation (RT50) at 1 Hz (p = 0.0028).
- (K) Representative sequence of HC-RP group to measure post-rest potentiation and diastolic excess fraction as the ratio between 3 Hz and 1Hz diastolic baselines.
- (L) Representative LC-RP data sequence.
- (M) Post-rest potentiation (p = 0.0049).
- (N) Diastolic excess fraction (p = 0.0325).
- (0) Sample Fura-2 Ca2+ transients at 1 Hz.
- (P) Fura-2 Ca2+ transient signal intensity at 1 Hz (p = 0.0248).
- (Q) Ca2+ transient decay time constant from peak to 80% relaxation (τ 80, p < 0.0001). Two way ANOVA with repeated measures (D–G) and unpaired two-tailed t tests (I, J, M, N, P, Q) were performed. *p < 0.05, **p < 0.005, ***p < 0.001, ****p < 0.0001.



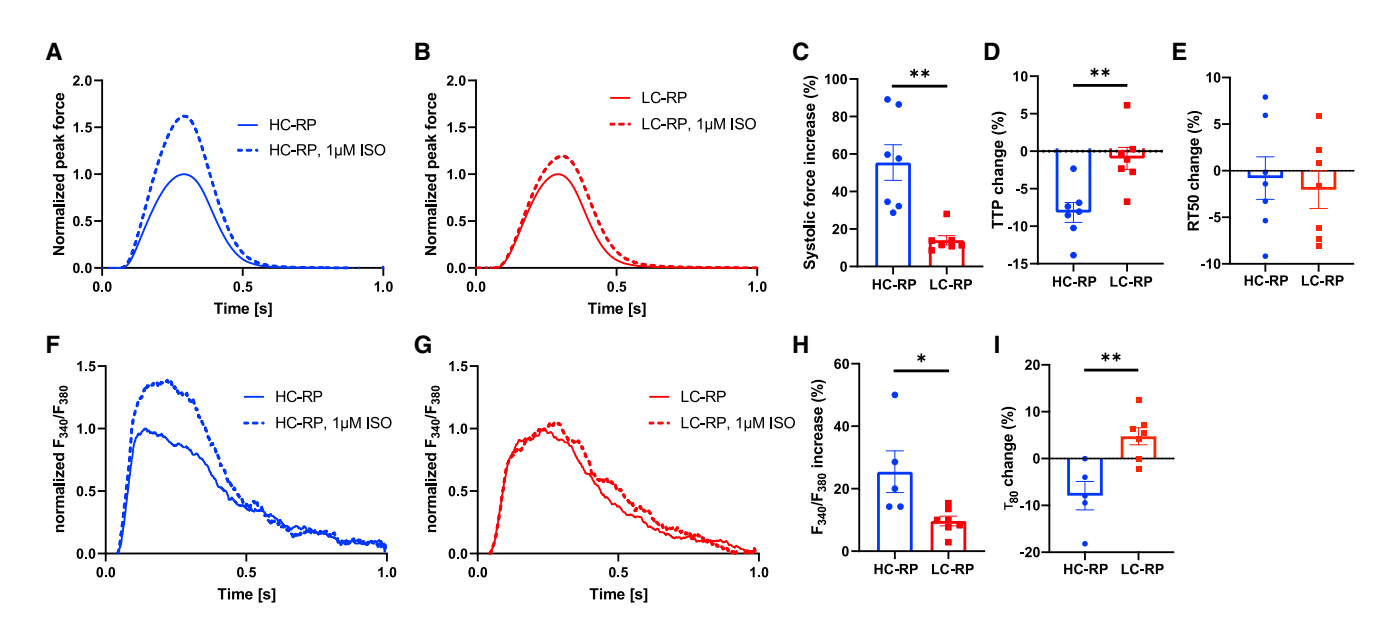


Figure 3. Physiological level Ca^{2+} and pacing result in improved β -adrenergic response to ISO

(A and B) Representative normalized HC-RP and LC-RP twitches at 1 Hz before and after 1 μM ISO infusion.

- (C) Systolic force increases in percentage (both n = 7, p = 0.0012).
- (D) TTP changes in percentage (both n = 7, p = 0.0033).
- (E) RT50 change in percentage (both n = 7).
- (F and G) Representative normalized HC-RP and LC-RP tissue Ca²⁺ transients with Fura-2 before and after ISO infusion.
- (H) Ca^{2+} transient intensity increases (HC-RP n = 5, LC-RP n = 7, p = 0.0223).
- (I) Ca²⁺ transient time decay constant from peak to 80% relaxation (τ_{80} , HC-RP n = 5, LC-RP n = 7, p = 0.0035). Unpaired two-tailed t-tests were performed for panels (C, D, H, and I). *p < 0.05, **p < 0.005. All data came from one differentiation batch.

more rapid character of isometric twitches in HC-RP compared with LC-RP tissue (Figures 2H-2J).

Post-rest potentiation was also assessed in HC-RP versus LC-RP tissues (Figures 2K and 2L). HC-RP tissue demonstrated significantly higher post-rest potentiation and smaller diastolic excess fraction (Figures 2M and 2N). Finally, to further confirm the Ca²⁺-handling differences between the two groups, Ca²⁺ transient measurements with FURA-2AM were performed. HC-RP EHTs showed lower fluorescent signal intensity change (Ca²⁺ transient amplitude) compared with LC-RP tissues (Figure 2O). A calculated decay time constant to 80% relaxation (τ_{80}) showed a highly significant improvement in Ca²⁺ reuptake rate for HC-RP tissues (Figure 2P).

To investigate the mechanistic underpinnings of the functional improvements shown in HC-RP tissues, we performed acute β-adrenergic response tests for both HC-RP and LC-RP EHTs. After the tissues had stabilized in the testing setup, EHTs were superfused with 1 μM isoproterenol (ISO) at 0.4 mL/min. The twitches at 1 Hz constant pacing were recorded every 40 s for 10 min until force stabilized. Representative normalized HC-RP twitches before and after ISO addition showed visible improvement in positive inotropic response to β-adrenergic stimulation compared with the RPMI group (Figures 3A and 3B). The systolic

peak force increase was significantly larger for HC-RP compared with LC-RP (Figure 3C). In addition, the HC-RP group showed a significantly decreased TTP in response to ISO (Figure 3D). Both groups exhibited a similar shortening of RT50 (Figure 3E). Moreover, HC-RP showed greater Ca²⁺ handling changes in response to β-adrenergic stimulation, as shown by the HC-RP's representative normalized Ca²⁺ transient intensity increase after ISO compared with limited changes seen in LC-RP (Figures 3F and 3G). HC-RP's higher Ca^{2+} transient intensity increase and faster τ_{80} were both significant (Figures 3H and 3I). Altogether, the HC-RP group displayed a more potent β-adrenergic response.

To understand the enhanced HC-RP response to ISO, myofilament and Ca²⁺ handling-related protein expression and composition were examined using western blots for sarcoplasmic reticulum Ca²⁺-ATPase (SERCA), phospholamban (PLN), phosphorylated PLN (p-PLN), cardiac troponin I (cTnI), and phosphorylated cTnI (p-cTnI). Sarcomere content measured with tropomyosin 1 (TPM1) remained similar between HC-RP and LC-RP (Figure 4A). Blots revealed significantly higher SERCA expression in LC-RP EHTs (Figure 4A), significantly higher PLN in HC-RP, marginally higher p-PLN in LC-RP (Figure 4B), and highly elevated cTnI and p-cTnI expression in HC-RP (Figure 4C).



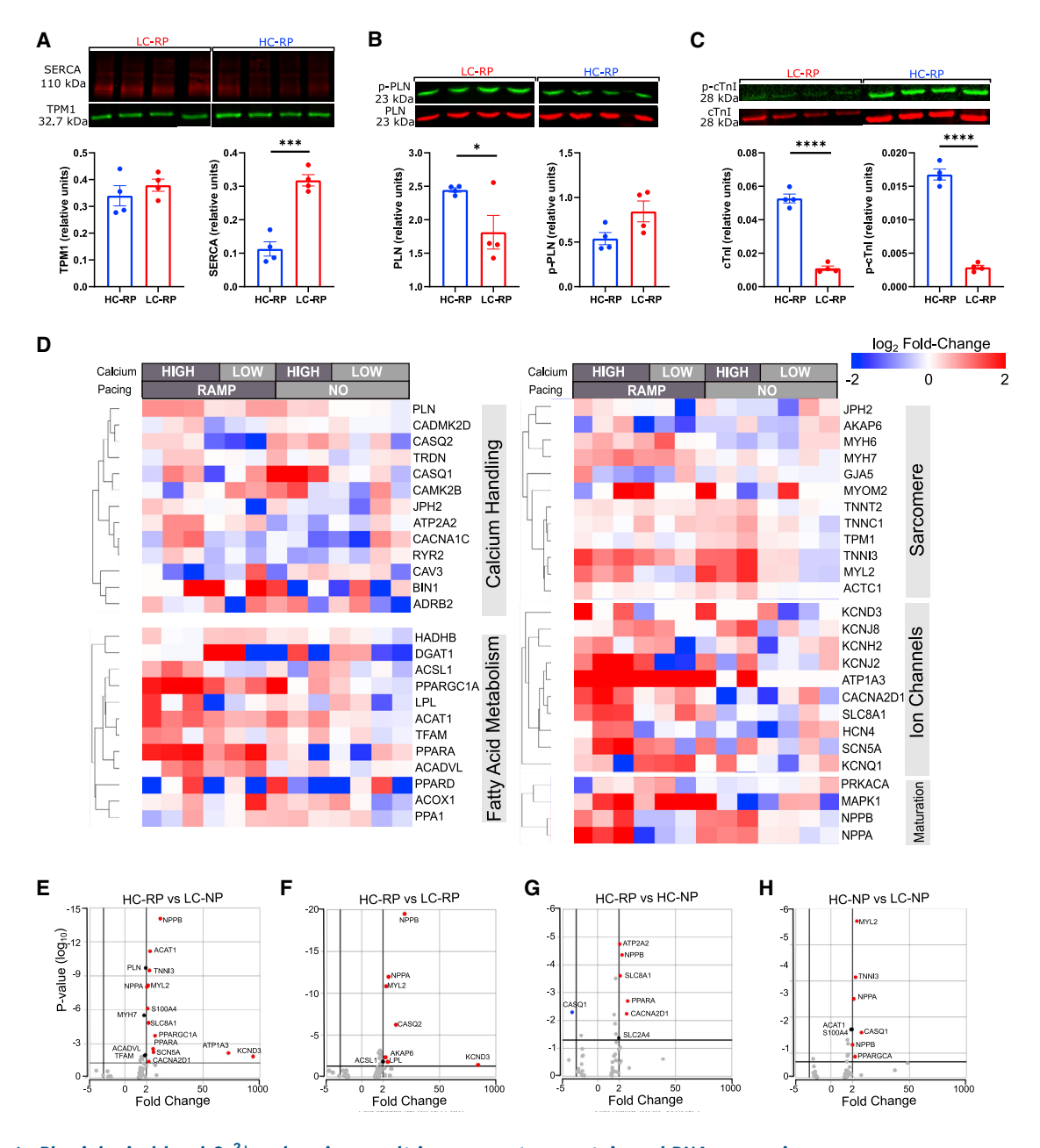
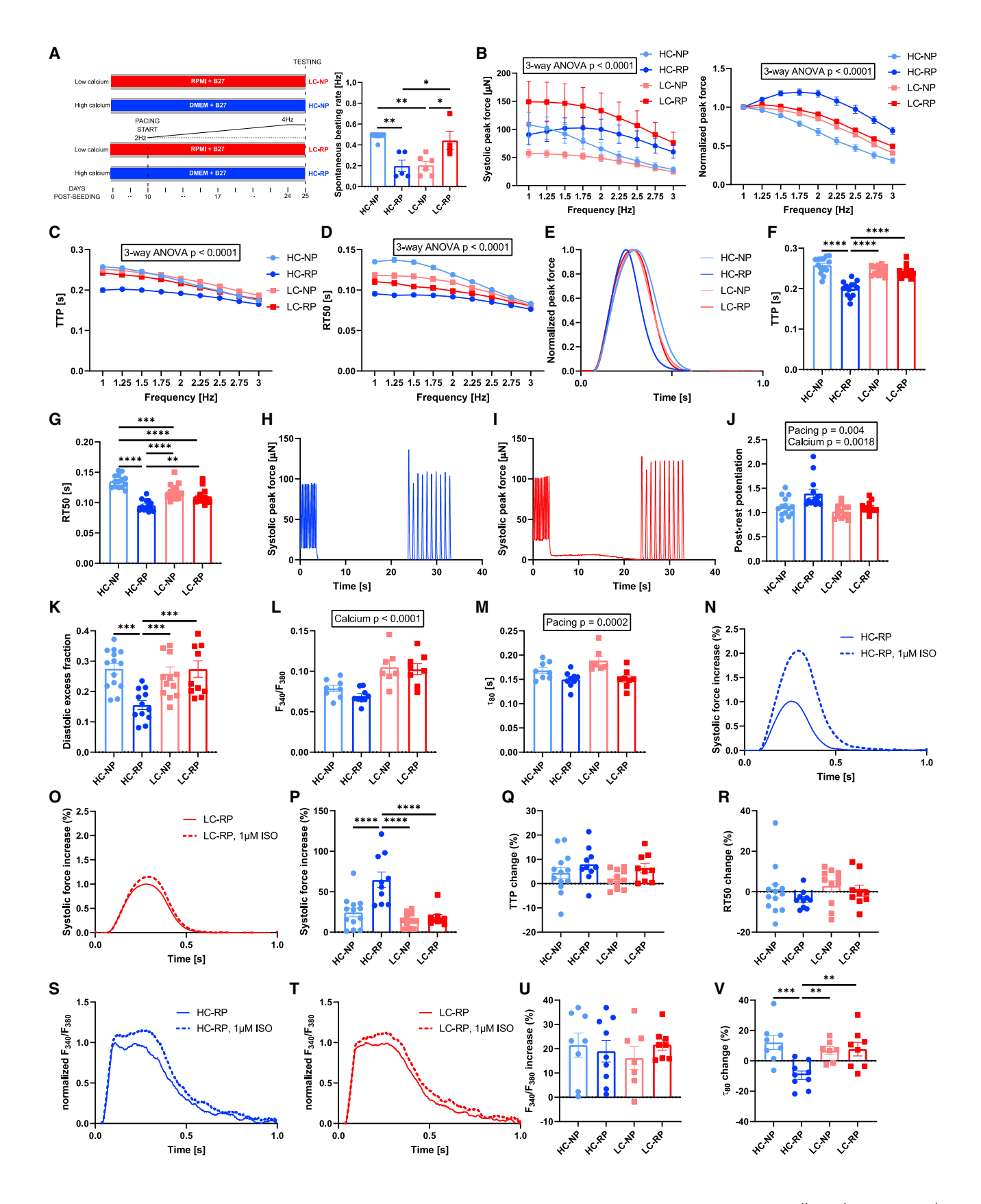


Figure 4. Physiological level Ca²⁺ and pacing result in more mature protein and RNA expression

All protein and RNA samples were extracted from tissues fresh frozen immediately after pacing. For western data, n = 4 for both groups and all measurement and ratios were first normalized against total protein. For RNA-seq, HC-RP n = 4, LC-RP n = 3, HC-NP n = 3, and LC-NP n = 4. Both western blotting and RNA-seq data came from one separate differentiation batch of the same single cell.

- (A) TPM1 and SERCA content (p = 0.0003).
- (B) PLN (p = 0.0477) and p-PLN.
- (C) cTnI (p < 0.0001) and p-cTnI (p < 0.0001).
- (D) RNA expression comparisons for Ca²⁺-handling proteins, sarcomere proteins, fatty acid metabolism, ion channels, and maturation markers.
- (E) HC-RP versus LC-NP volcano plot.
- (F) HC-RP versus LC-RP.
- (G) HC-RP versus HC-NP.
- (H) HC-NP versus LC-NP. Unpaired two-tailed t-tests were performed for (A–C). *p < 0.05, ***p < 0.001, ****p < 0.0001.







Additionally, RNA sequencing (RNA-seq) was carried out on a new set of conditioned tissues representing each of the four groups. Ca²⁺ concentration in the culture medium (irrespective of pacing) accounted for 341 differentially expressed genes, while the effect of ramp pacing (irrespective of culture medium) was associated with 653 gene expression differences ($|log(fold\ change)| > log(2)$, p < 0.05) (Figures S1A and S1B). RNAs of interest were further categorized into Ca²⁺ handling, sarcomere proteins, fatty acid metabolism, ion channels, and maturation markers. A comparison of HC-RP relative to LC-NP EHTs (the most extreme difference in culture conditions) (Figure 4E) showed significant changes in expression of genes relating to calcium handling ($\uparrow S100A4$, $\uparrow CACNA2D1$), the sarcomere (\uparrow TNNI3, \uparrow MYL2), ion channels (\uparrow SLC8A1, \uparrow SCN5A, \uparrow ATP1A3, and \uparrow KCND3), metabolism (↑ PPARGC1A, ↑ PPARA), and maturation (\uparrow NPPA, \uparrow NPPB). HC-RP versus LC-RP (Ca²⁺ effect in the presence of pacing, Figure 4F) showed expression changes related to Ca^{2+} handling ($\uparrow CASQ2$, $\uparrow AKAP6$), ion channels (\uparrow KCND3), the sarcomere (\uparrow MYL2), and maturation (↑ NPPA, ↑ NPPB). Comparing HC-RP relative to HC-NP (Pacing effect under high Ca2+, Figure 4G) showed changes in expression of genes relating to Ca²⁺ handling (\uparrow ATP2A2, \uparrow CACNA2D1, and \downarrow CASQ1), ion channel (\uparrow *SLC8A1*), metabolism ($\uparrow PPARA$), and maturation ($\uparrow NPPB$). Last, HC-NP versus LC-NP (Ca²⁺ effect alone, Figure 4H) included changes to Ca²⁺ handling (\uparrow *CASQ1*), sarcomere-(\uparrow *MYL2*, \uparrow *TNNI3*), metabolism-(\uparrow *PPARGC1A*), and maturation-(\uparrow *NPPA*, \uparrow *NPPB*) related genes.

To further validate that the functional improvement we saw in the healthy control line was not cell-line dependent, the complete suite of FFR and ISO response experiments was repeated in a different healthy control line from three separate differentiation batches for all four conditioning groups (Figure 5A). Only the HC-RP group showed positive FFR behavior, similar to that observed previously (Figure 5B), and HC-RP had the fastest TTP and RT50 across 1-3 Hz (Figures 5C and 5D). HC-RP significantly affected twitch kinetics at the baseline frequency of 1 Hz (Figure 4E), displaying a faster TTP and RT50 (Figures 5F and 5G). HC-RP was the only group with consistent post-rest potentiation (Figures 5H–5J) and significantly decreased diastolic excess fraction (Figure 5K). Ca²⁺ transients showed a higher signal intensity for both low-Ca²⁺ groups (Figure 5L). The Ca²⁺ transient decay constant showed a similar improvement for both ramp-pacing groups (Figure 5M). For adrenergic response to ISO, HC-RP showed a highly increased positive inotropy (Figures 5N-5P). All groups had insignificant TTP and RT50 changes (Figures 5Q and 5R). Last, all groups showed similar Ca²⁺ transient intensity increase (Figures 5S-SU), and HC-RP was the only group with a faster decay constant in response to ISO (Figure 5V).

Figure 5. Functional improvements from high calcium and ramp pacing were observed in a second iPSC line

(A) Two-way ANOVA experimental design (high Ca^{2+} vs. low Ca^{2+} ; ramp vs. no pacing) and spontaneous beating rate after ramp completion (two-way ANOVA p < 0.0001). Mechanical data (B-K) were from three separate differentiation batches (HC-NP n = 14, HC-RP n = 13, LC-NP n = 14, and LC-RP n = 12). FURA data (M, N, and T-W) were from two batches (n = 8, 9, 7, and 8, respectively). ISO data were from three batches (n = 13, 10, 11, and 9, respectively).

- (B) Raw and normalized FFR (p < 0.0001).
- (C) TTP from 1 to 3 Hz.
- (D) RT50.
- (E) Sample normalized peak force at 1 Hz.
- (F) TTP at 1 Hz (two-way ANOVA p = 0.0002, HC-RP vs. all others p < 0.0001).
- (G) RT50 at 1 Hz (two-way ANOVA p < 0.0001, HC-NP vs. LC-NP p = 0.0003, HC-NP vs. LC-RP p < 0.0001, HC-NP vs. HC-RP p < 0.0001, HC-RP vs. LC-RP p = 0.0018).
- (H and I) Raw post-rest potentiation data for HC-RP and LC-RP.
- (J) Post-rest potentiation.
- (K) Diastolic excess fraction (two-way ANOVA p < 0.0019, HC-RP vs. HC-NP p = 0.0001, HC-RP vs. LC-NP p = 0.0009, HC-RP vs. LC-RP p = 0.0003).
- (L) Ca²⁺ transient signal intensity.
- (M) Ca^{2+} transient decay (τ_{80}) .
- (N and 0) Sample HC-RP and LC-RP force responses to 1 μ M ISO.
- (P) Summary force changes to 1 μ M ISO (two-way ANOVA p = 0.004, HC-RP vs. all others p < 0.0001).
- (Q) TTP changes to ISO.
- (R) RT50 changes to ISO.
- (S and T) Example HC-RP and LCRP Ca^{2+} transients in response to 1 μ M ISO.
- (U) Ca²⁺ transient intensity changes to ISO.
- (V) τ_{80} changes to ISO (two-way ANOVA p = 0.0058, HC-RP vs. HC-NP p = 0.0003, HC-RP vs. LC-NP p = 0.0053, HC-RP vs. LC-RP p = 0.0025). Three-way ANOVA with repeated measures was performed for (B–D), two-way ANOVA with planned comparisons for (F, G, J–M, P–R, U, and V). **p < 0.001, ***p < 0.001, ****p < 0.0001.



DISCUSSION

Here we present a scalable advance in the maturation of iPSC-CMs, namely, growth of EHTs under conditions of physiological Ca²⁺ and ramp pacing. As far as we are aware, this is the first study that systematically examines the role of Ca²⁺ in cardiomyocyte maturation. In combination with ramp pacing, physiological Ca²⁺ led to functional characteristics that are realistically comparable with those of adult human ventricular myocardium, particularly in terms of their FFR, twitch kinetics, adrenergic responsiveness, and high expression and phosphorylation of the key regulatory myofilament isoform cTnI.

Healthy human myocardium typically exhibits a positive FFR up to 2-2.5 Hz (Chung et al., 2018a; Mulieri et al., 1992), similar to the behavior shown by HC-RP group in this study. At the same time, isometric twitch kinetics reported here (TTP of approximately 290 ms, RT50 at 120 ms) are similar to that of human trabeculae as well, with human TTP at approximately 200 ms and RT50 at approximately 120 ms (Chung et al., 2018b; Frank et al., 1998; Hasenfuss et al., 1994, 1996). In comparison, previous studies that combined supraphysiological (up to 6 Hz) ramp pacing and lower Ca²⁺ level possess unusually robust positive FFR up to 3–6 Hz and extremely fast kinetics (TTP and RT50 as low as 120 ms and 70 ms, respectively) (Ronaldson-Bouchard et al., 2018; Zhao et al., 2019).

Interestingly, one study has reported achievement of a positive FFR in EHTs without requiring electrical pacing in culture (Tiburcy et al., 2017). EHTs in that case were cultured in IMDM media (nominally 1.49 mM Ca²⁺), possibly leveraging some of the gene expression changes associated with higher Ca²⁺ we uncover in this study. Other possible factors contributing to the observed positive FFR are their use of antibiotics in culture (reported to reduce L-type Ca²⁺ current and intracellular Ca²⁺) (Belus and White, 2001, 2002), a number of additional factors (insulin-like growth factor-1, fibroblast growth factor-2, vascular endothelial growth factor, and transforming growth factorβ1), and possibly the specific cell line used. It is conceivable that, for certain cell lines, near physiological Ca²⁺ concentrations in media are sufficient to produce a positive FFR. However, this was certainly not the case in the two different iPSC lines that we examined, both of which showed a negative FFR, even under HC-NP conditions. The combination of high Ca²⁺ and pacing conditions seems to be a more reliable way of promoting positive FFR, independent of the specific cell line.

Other maturation strategies have attempted more complex media formulations, with, for example, hormones and fatty acids. Such protocols often prolong experiments to a time frame of several months, and, with or without a pacing protocol, these media formulations have not led to the maturation of twitch, Ca²⁺, β-adrenergic, and FFR maturation to levels we observed here (Birket et al., 2015; Feyen et al., 2020; Funakoshi et al., 2021; Gomez-Garcia et al., 2021; Jackman et al., 2018; de Lange et al., 2021; Pakzad et al., 2021: Rupert and Coulombe, 2017).

Moreover, RNA-seq shows upregulation in genes for Ca²⁺ handling, ion channels, sarcomere, fatty acid metabolism, and maturation in response to higher Ca²⁺ and ramp pacing compared with the baseline control in low Ca²⁺ and no pacing. These differentially expressed genes are helpful to understand the improved functional results in HC-RP in terms of FFR, contractile kinetics, post-rest potentiation, and enhanced β-adrenergic response. Interestingly, high Ca²⁺ alone (Figure S1C) can induce expressions in sarcomere ($\uparrow MYL2$, $\uparrow TNNI3$), Ca²⁺ handling ($\uparrow CASQ2$, \uparrow CASQ1), metabolism (\uparrow PPARGC1A), and maturation (\uparrow NPPA, ↑ NPPB). Ramp pacing itself (Figure S1D) also upregulates Ca²⁺ handling († CACNA2D1), ion channels (\uparrow ATP1A3), and metabolism (\uparrow PPARA). Furthermore, the addition of both high Ca2+ and ramp pacing together shows additional upregulated Ca^{2+} handling († S100A4), sarcomere (\uparrow TNNI3), ion channels (\uparrow SCN5A, \uparrow KCND3, \uparrow SLC8A1), and hypertrophy (\uparrow ACTA1) genes, suggesting synergy between physiological Ca²⁺ and ramp pacing in driving toward a more mature phenotype.

It was also noted that the maturation and hypertrophy markers NPPA, NPPB, and ACTA1 (Ronaldson-Bouchard et al., 2018) have higher expression in the HC-RP group relative to all others. To understand if this indicates physiological hypertrophy in myocyte growth and development, an analysis of genes in the P13K-Akt signaling pathway was conducted; Akt is reported to be critical in modulating physiological hypertrophy (DeBosch et al., 2006; Walsh, 2006). Akt is upregulated in HC-RP versus LC-RP (Figure S1E), but not for HC-NP versus LC-NP (Figure S1F), suggesting that the specific combination of high Ca²⁺ and ramp pacing promotes physiological growth in this instance.

To further assess our maturation progress, an analysis was performed to benchmark to human hearts and other maturation studies. We compared our data against RNA-seq data from Mills et al. (engineered three-dimensional [3D] tissues with maturation media) (Mills et al., 2017), Zhao et al. (engineered tissues with rapid pacing) (Zhao et al., 2019), and Sim et al. (adult, young and fetal ventricular samples from 21 human donors) (Sim et al., 2021). We obtained a common set of genes present in all four datasets, which was then used to perform principal component analysis (Figures S2A and S2B). From our analysis, we observed that samples from studies using engineered tissues clustered together and had less variability in terms of gene expression compared to donor samples from Sim et al.



(2021). We identified principal component 3 to be representative of the combination of a set of genes that was able to distinguish between the degrees of maturation between the tissues. To further confirm the comparability of our data, we picked 50 relevant cardiac genes and plotted the relative fold change of the treatment/most mature group with respect to the control/least mature group for each study (Figure S2C). The three EHT datasets exhibited fold changes in many genes that agreed with those of maturing human ventricular samples, but there were also several exceptions. The overall impression is one of continuing progress toward *in vitro* maturation of iPSC-CMs with the possibility of further gains in the future.

Among the results of these studies, we note some surprising data that deserve further discussion. Among tissues of both cell lines, those cultured in low Ca²⁺ media exhibited greater intracellular Ca²⁺ transients when tested (Figures 1P and 4L), with the latter confirming Ca²⁺ as the only significant factor affecting Ca^{2+} transient amplitude (p < 0.0001). It is important to recognize that low- and high-Ca²⁺ conditioned tissues were both characterized in the same Tyrode's solution (1.8 mM Ca²⁺) after 25 days in culture. The elevated Ca²⁺ transient amplitude in low Ca²⁺-conditioned tissues may indicate avid Ca²⁺ uptake when they are suddenly exposed to the higher Ca²⁺ concentration of Tyrode's solution during measurement. This is consistent with immature cardiomyocytes' increased dependence on extracellular Ca²⁺ through sarcolemmal Ca2+ influx to activate contraction (Louch et al., 2015; Vornanen, 1996). Moreover, RNA-seq comparisons between high and low Ca²⁺ conditions reveal elevated expression of CASQ1 and CASQ2 in high Ca2+ groups (Figure S2C), further suggesting low Ca²⁺ groups' more limited capability to store Ca²⁺ in the SR (sarcoplasmic reticulum). The seeming ability of physiological Ca²⁺ to promote SR maturation is an important implication of our study and merits further investigation.

Beyond functional maturation, the presence of cTnI and phosphorylation of cTnI has long proven to be an obstacle in cardiomyocyte maturation, with genetic engineering being used to artificially induce the isoform switch (Bedada et al., 2014; Wheelwright et al., 2020). In this work, we recognize that a hallmark of the FFR, which in an intact heart is a feature of β -adrenergic regulation, is not only the augmentation of systolic force, but also the decrease and maintenance of a low diastolic force at higher frequency with higher Ca²⁺ levels in the cells (Varian et al., 2009; Wiegerinck et al., 2009). Indeed, it appears that cTnI phosphorylation is crucial in promoting lusitropy by desensitizing the myofilament during increased contractile frequency (Nixon et al., 2012). In the HC-RP tissues in the present study, higher levels of cTnI expression and cTnI phosphorylation correlate well with their ability to present a realistic systolic and diastolic response to higher frequency of stimulation and robust β -adrenergic response (Li et al., 2000). Furthermore, cTnI is exclusively expressed in mature adult cardiomyocytes (Bedada et al., 2016; Sasse et al., 1993; Thijssen et al., 2004), and previous reports show less than 2% TnI is cTnI after 9.5 months of hiPSC-CM culture (Bedada et al., 2014). Therefore, the upregulation of TNNI3 seen in RNA-seq and western blot data confirm that our study provides a fast and effective method to increase cTnI expression.

In addition, our study reveals that calcium and pacing leads to interesting changes to Ca²⁺-handling proteins. HC-RP tissues exhibit higher PLN, lower p-PLN, and lower SERCA2 content compared with the LC-RP group. Although SERCA western blot results are lower in HC-RP compared with LC-RP, this may suggest post-translational modification or that SERCA activity is alternatively modulated through increased PLN phosphorylation (Figure 4B) and CASQ2 and AKAP6 upregulation (Figure 4F) for the same HC-RP versus LC-RP comparison. However, the exact reason for lower SERCA protein expression in HC-RP may warrant additional investigation. Nevertheless, the resulting higher PLN-to-SERCA2 ratio may indicate greater Ca²⁺-handling control and more headroom for SERCA2 activation via PLN phosphorylation. This is consistent with previous reports that increased PLN and decreased SERCA2 lead to augmented FFR (Bluhm et al., 2000; Meyer et al., 1999). The notion of enhanced headroom in the HC-RP tissues also seems to explain the more robust β-adrenergic response in both Ca^{2+} release and twitch force. Moreover, although the LC-RP group has significantly higher SERCA2 and higher p-PLN/PLN ratios, factors that should contribute to greater SERCA2 activation and faster cardiac relaxation (Meyer et al., 1999), twitch relaxation in this group (RT50) is actually much slower compared with the HC-RP group. This suggests that greater SERCA2 activity is not sufficient to overcome the lack of p-cTnI/cTnI in terms of efficient twitch relaxation. Collectively, the western blot results seemed to indicate that physiological Ca²⁺ and pacing made HC-RP group more efficient in handling Ca²⁺ and created significantly more headroom in PLN phosphorylation and subsequent SERCA activation, and a greater ability to phosphorylate cTnI under β-adrenergic stimulus compared with the LC-RP group.

Finally, some limitations of this work should be acknowledged. Although our intention was to develop a method with commercially available media and supplements for easy adoption, we recognize that there are compositional differences besides Ca²⁺ concentration between the high-glucose DMEM and RPMI with ATCC modification used in this study (Table S1). A comparison between the major components of the two media formulations shows the same K⁺ and glucose (5.33 and 1.80 mM, respectively),



but differences exist between DMEM and RPMI in total amino acids (10.7 mM vs. 6.6 mM, respectively), total concentration of various vitamins (0.15 mM vs. 0.24 mM, respectively), Na⁺ (155.3 mM vs. 128.0 mM, respectively), and Mg²⁺ (0.81 mM vs. 0.41 mM, respectively). Although the most significant difference remains in Ca²⁺ (1.8 mM vs. 0.42 mM, respectively), the additional differences could have also contributed to the functional, transcriptional, and protein differences observed in this study and may warrant further investigation. Last, albumin in the form of bovine serum albumin (BSA) is an important Ca²⁺-binding protein and critically affects the free Ca2+ concentration available to the tissues. RPMI- and DMEM-based media in our study only have BSA (fatty acid free fraction V) from B-27 at the same concentration, and, therefore, have no relevant impact on the final Ca²⁺ concentration. In any case, this does not detract from our principal finding, namely, that the combination of pacing and culture in DMEM constitutes a robust protocol for enhancing maturation in EHTs.

Furthermore, this is noted for the same HC-NP versus LC-NP comparison (Figures 1B and 5B), high Ca²⁺ improved twitch force. For the same HC-RP versus LC-RP comparison as the first control line (Figure 2D), high Ca²⁺ and pacing did not improve raw twitch force. This showed that the raw twitch force development by Ca²⁺ is cell line specific. However, we did not observe batch-to-batch variation of this behavior within the second cell line. This points to the inherent variability of force development between different cell lines under the same pacing condition, suggesting that cell line-specific pacing condition optimization may be required to ensure consistent twitch force development.

While the work shown here demonstrates specific gains in functional maturation, it must be acknowledged that it does not constitute a technique for achieving comprehensive cardiomyocyte maturity. Conspicuously, we have not investigated additional gains that may be made achieved by providing EHTs with a more realistic metabolic substrates, as others have done (Feyen et al., 2020; Yang et al., 2019). Future work will investigate the use of fatty acid-containing media in combination with HC-RP conditions. Nonetheless, we believe that HC-RP conditioning contributes meaningfully to the body of iPSC-CM maturation techniques because of its minimal complexity and shortening of the overall timeline to produce EHTs of acceptable maturity.

EXPERIMENTAL PROCEDURES

Reagents

High-glucose Dulbecco's Modified Eagle Medium (DMEM) and RPMI 1640 Medium (ATCC modification), B-27 supplements with and without insulin, TrypLE, Dulbecco's PBS (DPBS), fetal

bovine serum (FBS), penicillin-streptomycin (P/S), non-essential amino acids (NEAA), G-glutamine, and sodium pyruvate were purchased from ThermoFisher Scientific. CHIR99021, IWP4, and mTeSR were from STEMCELL Technologies. FURA 2/AM and ISO were from Sigma-Aldrich. Primary antibodies included SERCA2 (Invitrogen MA3-910), cTnI (Proteintech 66376-1-IG), *p*-cTnI (Cell Signaling Technology 4004S), *p*-PLN (Invitrogen PAS-38317), PLN (Invitrogen MA3-922), and TPM11 (Invitrogen PAS-29846). Secondary antibodies were from Bio-Rad.

EHT production

Decellularized porcine scaffolds to make EHTs were prepared as previously reported (Schwan et al., 2016). Briefly, fresh pig hearts (J Latella & Sons) were preserved in cold DPBS with 5% P/S until left ventricular free walls were cut into blocks and frozen on dry ice. Frozen blocks were sectioned into 150- μ m slices with a cryostat microtome (Leica CM3050 S) and laser cut into 2.5 × 6 mm scaffolds. The scaffolds were then incubated in lysis buffer (10 mM Tris and 0.1% 0.5 M EDTA in de-ionized [DI] water) and decellularization buffer (0.5% w/v SDS in DPBS). The scaffolds were affixed to laser-cut polytetrafluoroethylene holders and incubated overnight in incubation media (10% FBS and 2% P/S in DMEM) before seeding.

Cardiomyocyte differentiation

hiPSC-CMs differentiation followed commonly used protocol (Lian et al., 2013). Healthy control hiPSC line PGP1 (GM23338, Coriell Institute) was differentiated with 15 μ M CHIR99021 on day 0 for 24 h and 5 μ M IWP4 on day 3 for 48 h. On day 12, 4-day treatment with 4 mM lactate was used to purify hiPSC-CMs before cells were seeded on day 18. A second healthy control line was generated from monocytes in a peripheral blood sample of a healthy adult male and differentiated with 17.5 μ M CHIR99021 on day 0. The same differentiation protocol was followed after day 0 to day 14, after which the cells were expanded (Maas et al., 2021) with 2.4 μ M CHIR99021 on day 1, 3, and 5 after expansion. The media were switched back to RPMI + B27 Plus on day 6 with media change every other day until seeding on day 10.

For seeding, 1 million cells of 90% hiPSC-CMs and 10% adult human cardiac fibroblasts (PromoCell 306-05A) were used per tissue in the seeding media (10% FBS, 1% P/S, 1% NEAA, 1% L-glutamine, and 1% sodium pyruvate in DMEM). After seeding, tissues were maintained in either DMEM or RPMI with B27 (with insulin) and media were changed every other day.

Electrical stimulation and biomechanical testing

A custom bioreactor was used to electrically stimulate EHTs. It was assembled with laser-cut Teflon frames and CNC machined graphite electrodes (Graphitestore) to fit on top of a 12-well plate. It was connected to an Arduino Uno microcontroller and printed circuit board to provide bipolar pulses to individual tissues over a 2-week period with continuous ramp from 2 to 4 Hz. We applied a 2.5-V/cm across individual tissues. The bioreactor was cleaned with 70% ethanol and DI water and autoclaved in 30 min gravity cycle twice before use. Cell culture media were changed every other day during pacing.



A custom experimental setup was used to measure the biomechanical properties and ${\rm Ca}^{2+}$ transients of EHTs. A 3D-printed testing bath with platinum wires and printed circuit board provided pacing and heating with continuous perfusion during testing. A force transducer and linear actuator holding the tissue enabled precise real-time isometric force measurement. Tyrode's solution (in mM: 140 NaCl, 5.4 KCl, 1.8 CaCl₂, 1 MgCl₂, 25 HEPES, and 10 glucose; pH 7.30) was used in testing. MATLAB scripts were used to record, process, and analyze mechanical data. Isometric twitches, FFR, post-rest potentiation, and ${\rm Ca}^{2+}$ transient recordings were conducted at 10% stretch.

Statistics

To compare the difference in biomechanical properties, ${\rm Ca}^{2+}$ transients, and protein expression levels between DMEM and RPMI groups, unpaired two-tailed t-tests (Figures 2, 3, and 4) and two-way ANOVA with repeated measures (Figure 2) were performed. All analyses were performed in GraphPad Prism 8 software and individual data points were presented whenever possible with means and SEM A p value of <0.05 was used for all analysis to be considered significant.

Western blot

The EHTs were flash frozen on dry ice and stored in −80°C freezer for up to 2 weeks. The proteins were homogenized in RIPA buffer supplemented with sodium orthovanadate, PMSF, protease inhibitor cocktail, and phosphatase inhibitor cocktail (Santa Cruz Biotechnology). The protein was separated on precast 4%–20% Mini-PROTEAN TGXgels (Bio-Rad) before transfer to a PVDF membrane (Millipore). Samples were normalized using Revert Total Protein Stain (Li-Cor). The membrane was incubated in primary antibodies overnight at 4°C. The membranes were imaged on a Li-Cor Odyssey scanner. Quantification and analysis were performed using Image Studio Lite software (Li-Cor).

RNA-seq

For RNA extraction, tissues were flash frozen and crushed with plastic pestles. Aqueous phase was collected after TRIzol (Ambion) phase separation, and the RNA pellets were precipitated for total RNA extraction. Samples were treated with DNAse and cleaned with Qiagen RNeasy columns.

Samples were sequenced by Yale Center for Genomic Analysis (Illumina HiSeq 2500, multiplexed, paired-end reads of 100 base pair length with 25 million reads per sample). Data analysis was performed on PartekFlow. Alignment was performed using STAR 2.7.8a and hg38 as the reference genome. Samples were clustered by average linkage using Pearson's dissimilarity. Fifty relevant genes were then selected to perform differential analysis using DESeq2 with p < 0.05 and fold change of ≤ -2 or ≥ 2 .

Pathway analysis was performed using the pathway enrichment functionality of Partek Flow software on a dataset of $\geq 15,000$ genes. Relevant pathways which had an enrichment score >5 and a p value of <0.05 were considered. For each pairwise comparison between treatment groups, relevant Kyoto Encyclopedia of Genes and Genomes pathways were visualized to make qualitative observations regarding the directionality of regulation of specific genes.

Data and code availability

The RNASeq data from this study are available under GEO accession ID: GSE201437.

SUPPLEMENTAL INFORMATION

Supplemental information can be found online at https://doi.org/10.1016/j.stemcr.2022.07.006.

AUTHOR CONTRIBUTIONS

All authors contributed to study design, data collection, data analysis, manuscript writing, and revision.

ACKNOWLEDGMENTS

We acknowledge the following sources of support: NIH R01HL136590 and NSF CAREER 1653160 to SGC; P.D. Soros Fellowship for New Americans, NIH/NIGMS Medical Scientist Training Program Grant (T32GM007205), and American Heart Association Predoctoral Fellowship to L.R.S.

CONFLICTS OF INTEREST

S.G.C. has equity ownership in Propria LLC, which has licensed EHT technology used in the research reported in this publication. This arrangement has been reviewed and approved by the Yale University Conflict of Interest Office. The authors declare no additional competing financial interests.

Received: July 27, 2021 Revised: July 8, 2022 Accepted: July 8, 2022 Published: August 4, 2022

REFERENCES

Bedada, F.B., Chan, S.S.K., Metzger, S.K., Zhang, L., Zhang, J., Garry, D.J., Kamp, T.J., Kyba, M., and Metzger, J.M. (2014). Acquisition of a quantitative, stoichiometrically conserved ratiometric marker of maturation status in stem cell-derived cardiac myocytes. Stem Cell Rep. *3*, 594–605.

Bedada, F.B., Wheelwright, M., and Metzger, J.M. (2016). Maturation status of sarcomere structure and function in human iPSC-derived cardiac myocytes. Biochim. Biophys. Acta *1863*, 1829–1838.

Belus, A., and White, E. (2001). Effects of antibiotics on the contractility and Ca2+ transients of rat cardiac myocytes. Eur. J. Pharmacol. *412*, 121–126.

Belus, A., and White, E. (2002). Effects of streptomycin sulphate on I(CaL), I(Kr) and I(Ks) in Guinea-pig ventricular myocytes. Eur. J. Pharmacol. *445*, 171–178.

Birket, M.J., Ribeiro, M.C., Kosmidis, G., Ward, D., Leitoguinho, A.R., van de Pol, V., Dambrot, C., Devalla, H.D., Davis, R.P., Mastroberardino, P.G., et al. (2015). Contractile defect caused by mutation in MYBPC3 revealed under conditions optimized for human PSC-cardiomyocyte function. Cell Rep. 13, 733–745.



Bluhm, W.F., Kranias, E.G., Dillmann, W.H., and Meyer, M. (2000). Phospholamban: a major determinant of the cardiac force-frequency relationship. Am. J. Physiol. Heart Circ. Physiol. *278*, H249–H255.

Chung, J.-H., Martin, B.L., Canan, B.D., Elnakish, M.T., Milani-Nejad, N., Saad, N.S., Repas, S.J., Schultz, J.E.J., Murray, J.D., Slabaugh, J.L., et al. (2018a). Etiology-dependent impairment of relaxation kinetics in right ventricular end-stage failing human myocardium. J. Mol. Cell. Cardiol. *121*, 81–93.

Chung, J.H., Canan, B.D., Whitson, B.A., Kilic, A., and Janssen, P.M.L. (2018b). Force-frequency relationship and early relaxation kinetics are preserved upon sarcoplasmic blockade in human myocardium. Physiol. Rep. *6*, e13898.

DeBosch, B., Treskov, I., Lupu, T.S., Weinheimer, C., Kovacs, A., Courtois, M., and Muslin, A.J. (2006). Akt1 is required for physiological cardiac growth. Circulation *113*, 2097–2104.

de Lange, W.J., Farrell, E.T., Kreitzer, C.R., Jacobs, D.R., Lang, D., Glukhov, A.V., and Ralphe, J.C. (2021). Human iPSC-engineered cardiac tissue platform faithfully models important cardiac physiology. Am. J. Physiol. Heart Circ. Physiol. *320*, H1670–H1686. https://doi.org/10.1152/ajpheart.00941.2020.

Feric, N.T., and Radisic, M. (2016). Maturing human pluripotent stem cell-derived cardiomyocytes in human engineered cardiac tissues. Adv. Drug Deliv. Rev. *96*, 110–134.

Feyen, D.A.M., McKeithan, W.L., Bruyneel, A.A.N., Spiering, S., Hörmann, L., Ulmer, B., Zhang, H., Briganti, F., Schweizer, M., Hegyi, B., et al. (2020). Metabolic maturation media improve physiological function of human iPSC-derived cardiomyocytes. Cell Rep. 32. 107925.

Frank, K., Bölck, B., Bavendiek, U., and Schwinger, R.H. (1998). Frequency dependent force generation correlates with sarcoplasmic calcium ATPase activity in human myocardium. Basic Res. Cardiol. *93*, 405–411.

Funakoshi, S., Fernandes, I., Mastikhina, O., Wilkinson, D., Tran, T., Dhahri, W., Mazine, A., Yang, D., Burnett, B., Lee, J., et al. (2021). Generation of mature compact ventricular cardiomyocytes from human pluripotent stem cells. Nat. Commun. *12*, 3155.

Gomez-Garcia, M.J., Quesnel, E., Al-attar, R., Laskary, A.R., and La-flamme, M.A. (2021). Maturation of human pluripotent stem cell derived cardiomyocytes in vitro and in vivo. Semin. Cell Dev. Biol. *118*, 163–171.

Hasenfuss, G., Holubarsch, C., Hermann, H.P., Astheimer, K., Pieske, B., and Just, H. (1994). Influence of the force-frequency relationship on haemodynamics and left ventricular function in patients with non-failing hearts and in patients with dilated cardiomyopathy. Eur. Heart J. *15*, 164–170.

Hasenfuss, G., Reinecke, H., Studer, R., Pieske, B., Meyer, M., Drexler, H., and Just, H. (1996). Calcium cycling proteins and force-frequency relationship in heart failure. Basic Res. Cardiol. *91*, 17–22. Jackman, C., Li, H., and Bursac, N. (2018). Long-term contractile activity and thyroid hormone supplementation produce engineered rat myocardium with adult-like structure and function. Acta Biomater. *78*, 98–110.

Li, L., Desantiago, J., Chu, G., Kranias, E.G., and Bers, D.M. (2000). Phosphorylation of phospholamban and troponin I in β -adren-

ergic-induced acceleration of cardiac relaxation. Am. J. Physiol. Heart Circ. Physiol. *278*, H769–H779.

Lian, X., Zhang, J., Azarin, S.M., Zhu, K., Hazeltine, L.B., Bao, X., Hsiao, C., Kamp, T.J., and Palecek, S.P. (2013). Directed cardiomyocyte differentiation from human pluripotent stem cells by modulating Wnt/ β -catenin signaling under fully defined conditions. Nat. Protoc. *8*, 162–175.

Louch, W.E., Koivumäki, J.T., and Tavi, P. (2015). Calcium signalling in developing cardiomyocytes: implications for model systems and disease. J. Physiol. *593*, 1047–1063.

Ma, N., Zhang, J.Z., Itzhaki, I., Zhang, S.L., Chen, H., Haddad, F., Kitani, T., Wilson, K.D., Tian, L., Shrestha, R., et al. (2018). Determining the pathogenicity of a genomic variant of uncertain significance using CRISPR/Cas9 and human-induced pluripotent stem cells. Circulation *138*, 2666–2681.

Maas, R.G.C., Lee, S., Harakalova, M., Snijders Blok, C.J.B., Goodyer, W.R., Hjortnaes, J., Doevendans, P.A.F.M., Van Laake, L.W., van der Velden, J., Asselbergs, F.W., et al. (2021). Massive expansion and cryopreservation of functional human induced pluripotent stem cell-derived cardiomyocytes. STAR Protoc. *2*, 100334.

Meyer, M., Bluhm, W.F., He, H., Post, S.R., Giordano, F.J., Lew, W.Y., and Dillmann, W.H. (1999). Phospholamban-to-SERCA2 ratio controls the force-frequency relationship. Am. J. Physiol. *276*, H779–H785.

Mills, R.J., Titmarsh, D.M., Koenig, X., Parker, B.L., Ryall, J.G., Quaife-Ryan, G.A., Voges, H.K., Hodson, M.P., Ferguson, C., Drowley, L., et al. (2017). Functional screening in human cardiac organoids reveals a metabolic mechanism for cardiomyocyte cell cycle arrest. Proc. Natl. Acad. Sci. USA *114*, E8372–E8381.

Mulieri, L.A., Hasenfuss, G., Leavitt, B., Allen, P.D., and Alpert, N.R. (1992). Altered myocardial force-frequency relation in human heart failure. Circulation *85*, 1743–1750.

Ng, R., Sewanan, L.R., Stankey, P., Li, X., Qyang, Y., and Campbell, S. (2021). Shortening velocity causes myosin isoform shift in human engineered heart tissues. Circ. Res. *128*, 281–283.

Nixon, B.R., Thawornkaiwong, A., Jin, J., Brundage, E.A., Little, S.C., Davis, J.P., Solaro, R.J., and Biesiadecki, B.J. (2012). AMP-activated protein kinase phosphorylates cardiac troponin I at Ser-150 to increase myofilament calcium sensitivity and blunt PKA-dependent function. J. Biol. Chem. *287*, 19136–19147.

Pakzad, K.K., Tan, J.J., Anderson, S., Board, M., Clarke, K., and Carr, C.A. (2021). Metabolic maturation of differentiating cardiospherederived cells. Stem Cell Res. *54*, 102422.

Pieske, B., Sütterlin, M., Schmidt-Schweda, S., Minami, K., Meyer, M., Olschewski, M., Holubarsch, C., Just, H., and Hasenfuss, G. (1996). Diminished post-rest potentiation of contractile force in human dilated cardiomyopathy functional evidence for alterations in intracellular Ca 2 handling. J. Clin. Invest. *98*, 764–776. Robertson, C., Tran, D.D., and George, S.C. (2013). Concise review: maturation phases of human pluripotent stem cell-derived cardiomyocytes. Stem Cell *31*, 829–837.

Ronaldson-Bouchard, K., Ma, S.P., Yeager, K., Chen, T., Song, L., Sirabella, D., Morikawa, K., Teles, D., Yazawa, M., and Vunjak-Novakovic, G. (2018). Advanced maturation of human cardiac tissue grown from pluripotent stem cells. Nature *556*, 239–243.



Rupert, C.E., and Coulombe, K.L.K. (2017). IGF1 and NRG1 enhance proliferation, metabolic maturity, and the force-frequency response in hESC-derived engineered cardiac tissues. Stem Cells Int. 2017, 7648409.

Sasse, S., Brand, N.J., Kyprianou, P., Dhoot, G.K., Wade, R., Arai, M., Periasamy, M., Yacoub, M.H., and Barton, P.J. (1993). Troponin I gene expression during human cardiac development and in endstage heart failure. Circ. Res. *72*, 932–938.

Schwan, J., Kwaczala, A.T., Ryan, T.J., Bartulos, O., Ren, Y., Sewanan, L.R., Morris, A.H., Jacoby, D.L., Qyang, Y., and Campbell, S.G. (2016). Anisotropic engineered heart tissue made from laser-cut decellularized myocardium. Sci. Rep. *6*, 32068.

Sewanan, L.R., and Campbell, S.G. (2020). Modelling sarcomeric cardiomyopathies with human cardiomyocytes derived from induced pluripotent stem cells. J. Physiol. *598*, 2909–2922.

Sim, C.B., Phipson, B., Ziemann, M., Rafehi, H., Mills, R.J., Watt, K.I., Abu-Bonsrah, K.D., Kalathur, R.K.R., Voges, H.K., Dinh, D.T., et al. (2021). Sex-specific control of human heart maturation by the progesterone receptor. Circulation *143*, 1614–1628.

Thijssen, V.L.J.L., Ausma, J., Gorza, L., Van Der Velden, H.M.W., Allessie, M.A., Van Gelder, I.C., Borgers, M., and Van Eys, G.J.J.M. (2004). Troponin I isoform expression in human and experimental atrial fibrillation. Circulation *110*, 770–775.

Tiburcy, M., Hudson, J.E., Balfanz, P., Schlick, S., Meyer, T., Chang Liao, M.L., Levent, E., Raad, F., Zeidler, S., Wingender, E., et al. (2017). Defined engineered human myocardium with advanced maturation for applications in heart failure modeling and repair. Circulation *135*, 1832–1847.

Tyser, R.C., Miranda, A.M., Chen, C.M., Davidson, S.M., Srinivas, S., and Riley, P.R. (2016). Calcium handling precedes cardiac differentiation to initiate the first heartbeat. Elife *5*, e17113.

Varian, K.D., Kijtawornrat, A., Gupta, S.C., Torres, C.A.A., Monasky, M.M., Hiranandani, N., Delfin, D.A., Rafael-Fortney, J.A., Periasamy, M., Hamlin, R.L., and Janssen, P.M.L. (2009). Impairment of diastolic function by lack of frequency-dependent myofilament desensitization in rabbit right ventricular hypertrophy. Circ. Heart Fail. *2*, 472–481.

Vornanen, M. (1996). Contribution of sarcolemmal calcium current to total cellular calcium in postnatally developing rat heart. Cardiovasc. Res. *32*, 400–410.

Walsh, K. (2006). Akt signaling and growth of the heart. Circulation 113, 2032–2034.

Wheelwright, M., Mikkila, J., Bedada, F.B., Mandegar, M.A., Thompson, B.R., and Metzger, J.M. (2020). Advancing physiological maturation in human iPSC-derived cardiac muscle by gene editing an inducible adult troponin isoform switch. Stem Cell *38*, 1254–1266.

Wiegerinck, R.F., Cojoc, A., Zeidenweber, C.M., Ding, G., Shen, M., Joyner, R.W., Fernandez, J.D., Kanter, K.R., Kirshbom, P.M., Kogon, B.E., and Wagner, M.B. (2009). Force frequency relationship of the human ventricle increases during early postnatal development. Pediatr. Res. *65*, 414–419.

Yang, X., Rodriguez, M.L., Leonard, A., Sun, L., Fischer, K.A., Wang, Y., Ritterhoff, J., Zhao, L., Kolwicz, S.C., Pabon, L., et al. (2019). Fatty acids enhance the maturation of cardiomyocytes derived from human pluripotent stem cells. Stem Cell Rep. *13*, 657–668.

Zhao, Y., Rafatian, N., Feric, N.T., Cox, B.J., Aschar-Sobbi, R., Wang, E.Y., Aggarwal, P., Zhang, B., Conant, G., Ronaldson-Bouchard, K., et al. (2019). A platform for generation of chamber specific cardiac tissues and disease modelling. Cell *176*, 913–927.e18.